JPE 13-3-16

http://dx.doi.org/10.6113/JPE.2013.13.3.479

Wireless Paralleled Control Strategy of Three-phase Inverter Modules for Islanding Distributed Generation Systems

Zhiqiang Guo*, Deshang Sha†, and Xiaozhong Liao*

*†School of Automation, Beijing Institute of Technology, Beijing, China

Abstract

This paper presents a control strategy for distributed systems, which can be used in islanded microgrids. The control strategy is based on the droop method, which uses locally measured feedback to achieve load current sharing. Instead of the traditional droop method, an improved one is implemented. A virtual inductor in the synchronous frame for three-phase inverters is proposed to deal with the coupling of the frequency and the amplitude related to the active and reactive power. Compared with the traditional virtual inductor, the proposed virtual inductor is not affected by high frequency noises because it avoids differential calculations. A model is given for the distributed generation system, which is beneficial for the design of the droop coefficients and the value of the virtual inductor. The effectiveness of the proposed control strategy is verified by simulation and experiment results.

Key words: Current sharing, Droop method, Inverter parallel, Mircogrid, Virtual inductors

I. INTRODUCTION

Distributed generation (DG) is widely used due to its higher efficiency, higher reliability and lower emission costs [1], [2]. Distributed generation systems are composed of many power sources such as fuel cells, photovoltaic cells, and wind turbines. They are called microgrids, and are becoming an increasingly important concept. In order to achieve flexibility, communication links should be eliminated among the constituent DG units, which can be located far away. As a result, the control regulation of the individual DG units should be achieved through their own feedback variables [2].

All DG units outputs should have the same phase and amplitude. Otherwise, the microgrid devices may be damaged due to uncontrollable power flow among the units. Compared with traditional inverters, the DG units tend to have a faster transient response. Once one of them fails, it should be disconnected from the microgrid. However, when it recovers, it can be reconnected to the system again. Therefore, the method used to achieve smooth hot swapping is very important.

In order to realize the control objectives, many control strategies have been proposed. Traditionally, the paralleled inverter modules communicate with each other to share the load power. A distributed generation system circuit model in a standalone AC power system is presented in [3]. Paralleled inverters for smooth mode transfer microgrid applications are introduced in [4]. As a microgrid is disconnected from the utility, one inverter working as the master operates in voltage source mode, while the other slave units work in current source mode. Once the microgrid connects to the utility, all of the units work in current source mode. If the master unit fails in island mode, the system can not operate normally. For inverters operating in parallel, sharing the load power is challenging because they should have the same frequency, phase, amplitude and even the same carrier waveform [5]. In order to share load currents equally, central control is widely used. However, it is not suitable for distributed generation systems in which the units are located far apart. However, the frequency/voltage droop control [6]-[17] allows the individual units to control their individual output voltages independently, without communications among each other.

Although the droop control is suitable for DG units, the traditional droop control method is not applicable to nonlinear loads [7]. Harmonic currents need to be shared as well. Several control strategies have been proposed to share the harmonic

Manuscript received Jul. 2, 2012; revised Feb. 10, 2013
Recommended for publication by Associate Editor Jaeho Choi.
†Corresponding Author: shadeshang@bit.edu.cn
Tel: +86-10-68918613, Beijing Institute of Technology
*School of Automation, Beijing Institute of Technology, China

currents properly. In [9], a control scheme is presented where nonlinear load currents can be shared equally by detecting the harmonic currents in three-phase inverter systems. In [10], harmonic currents sharing is achieved by adjusting the voltage references. The virtual inductor control strategy is widely used for paralleled inverter system to decouple the active and reactive power. However, all of the virtual inductor control strategies are implemented in the stationary α-β frame. Differential computation is necessary for these control strategies. However, high frequency noises can be amplified.

This paper presents a control strategy for three phase DG inverters. Compared with the traditional virtual inductance, an improved virtual inductance without differential calculations is proposed. Due to the lack of differential computations, the system is not sensitive to disturbances. Therefore, the proposed virtual inductance is more robust than the traditional one. A stability analysis is given for designing the droop coefficients and the virtual inductance. In the following sections, the fundamental control theory for connecting the AC power units in parallel is described firstly. Secondly, a virtual inductor implemented in the synchronous d-q frame is proposed to achieve accurate load current sharing. Thirdly, a model of the system is built to analyze its stability. Finally, simulations and experiments are conducted to verify the effectiveness of the proposed control strategy.

II. Review of Fundamental Droop Control

Fig. 1 shows a DG system composed of different sources. Each source is converted into a fundamental AC source and connected with a common AC bus. The equivalent circuit of a parallel AC source unit is shown in Fig.2, where $\overset{\mathbf{u}}{V} = V\angle 0°$ is the voltage of the common AC bus, $\overset{\mathbf{u}}{E} = E\angle\phi$ is the output voltage of the inverter unit, ϕ is the phase angle between the inverter and the common AC bus, $\overset{\mathbf{u}}{Z} = Z\cos\theta + j\cdot Z\sin\theta = R + j\cdot X$ is the transmission line impedance and θ is the phase angle of the transmission line impedance.

As seen from Fig.2, the apparent power drawn to the common AC bus can be expressed as:

$$\begin{aligned} S &= P + j\cdot Q = V\cdot I^{*} \\ &= V(\frac{E\angle\phi - V\angle 0^{\circ}}{\vec{Z}})^{*} = V(\frac{E\cdot e^{j\phi} - V}{\vec{Z}})^{*} \\ &= \frac{V(E\cos\phi - V)\cos\theta + EV\sin\phi\sin\theta}{Z} \\ &+ j\frac{V(E\cos\phi - V)\sin\theta - EV\sin\phi\cos\theta}{Z} \end{aligned} \tag{1}$$

where P and Q are the active and reactive power, respectively.

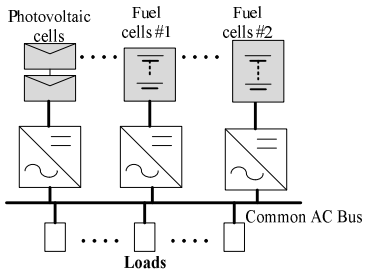

Fig. 1. Distributed generation system.

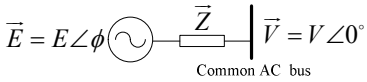

Fig. 2. Equivalent circuit of parallel AC source.

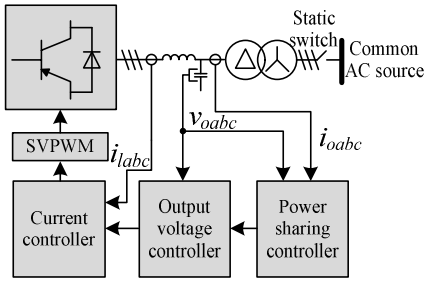

Fig. 3. Control block of the three-phase inverter unit.

From (1), P and Q can be expressed as follows:

$$\begin{cases} P = \dfrac{V(E\cos\phi - V)}{Z}\cos\theta + \dfrac{EV\sin\phi}{Z}\sin\theta \\ Q = \dfrac{V(E\cos\phi - V)}{Z}\sin\theta - \dfrac{EV\sin\phi}{Z}\cos\theta \end{cases} \tag{2}$$

Traditionally, φ is very small, so $\sin\phi \approx \phi$ and $\cos\phi \approx 1$. Therefore, based on (2), the following is obtained:

$$\begin{cases} V(E - V) = Z(P\cos\theta + Q\sin\theta) \\ EV\cdot\phi = Z(P\sin\theta - Q\cos\theta) \end{cases} \tag{3}$$

Thus the power angle depends predominantly on the active power P, whereas the amplitude of the output voltage depends predominantly on the reactive power Q, which is the traditional $P-\omega$ and $Q-E$ droop [8]. The control scheme can be expressed as the following:

$$\begin{cases} \omega = \omega^{*} - m\cdot P \\ E = E^{*} - n\cdot Q \end{cases} \tag{4}$$

where ω^{*} and E^{*} are the frequency and amplitude of the output voltage amplitude at no load, and m and n are the droop coefficients for the active power and the reactive power, respectively.

III. Analysis of the Back-EMF Estimator

The control strategy of the three-phase voltage source inverter is shown in Fig.3, where the three-loop control

scheme is designed. The outer control loop is designed to obtain power sharing among the inverter units. The middle control loop is the output voltage control loop whose reference is the output of the power sharing controller. The current loop works as the inner control loop.

A. Power Sharing Loop

Using the two-axis theory, the instantaneous active power p and reactive power q can be given by:

$$\begin{cases} p = u_d \cdot i_{od} + u_q \cdot i_{oq} \\ q = u_q \cdot i_{od} - u_d \cdot i_{oq} \end{cases} \tag{5}$$

where u_d, u_q and i_{od}, i_{oq} are the three-phase output voltages and the load currents obtained from the Park transformation, respectively. In order to allow for a sufficient time-scale separation between the power sharing loop and the voltage control loop [1], the active and reactive power of the fundamental components are obtained by a low-pass filter as follows:

$$\begin{cases} P = \dfrac{\omega_c}{s+\omega_c} p \\ Q = \dfrac{\omega_c}{s+\omega_c} q \end{cases} \tag{6}$$

where ω_c is the cutoff frequency of the low pass filter.

In the d-q synchronous rotating frame, the voltage reference of the inverter is expressed as $[v_{dref}\ v_{qref}]^{\mathrm{T}}=[V_{ref}\ 0]^{\mathrm{T}}$, where V_{ref} is the reference of the output voltage amplitude obtained from the Park transformation. Therefore, the $P-\omega$ and $Q-E$ method under d-q frame is written by:

$$\begin{cases} \omega = \omega^* - mP \\ v_{dref} = V_{ref} - nQ \\ v_{qref} = 0 \end{cases} \tag{7}$$

where ω^* is the angular speed set point. To improve the dynamic response, an improved control strategy based on the droop method is proposed in [1]. In synchronous frame, the control strategy can be expressed as:

$$\begin{cases} \omega = \omega^* - mP - m_d\, dP/dt \\ v_{dref} = V_{ref} - nQ - n_d\, dQ/dt \\ v_{qref} = 0 \end{cases} \tag{8}$$

where m_d and n_d are adaptive transient droop gains. With this strategy, the damping gain is adaptively tuned under different conditions. Furthermore, the dynamic response of the paralleled inverter can be improved effectively.

Actually, the transmission line contains resistance. The $P-\omega$ and $Q-E$ droops control is not effective when the output impedance is resistive. Besides, accurate power sharing depends on the output impedance. In order to improve the output impedance characteristics, a virtual inductor is proposed in [12], in which the output impedance is designed properly for the inverters to achieve accurate load current sharing and a reduction of the harmonic voltage distortion.

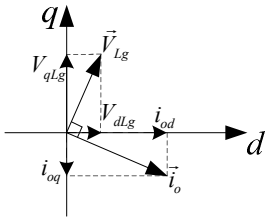

Fig. 4. Phase diagram in d-q frame.

For three-phase inverters transformed in the synchronous frame, the voltage and current vectors are depicted in Fig. 4. The voltage drop across the inductor $\vec{V}_{Lg}$ leads the current $\vec{i}$ by 90^0 and it is written by:

$$V_{dLg} + jV_{qLg} = j \cdot \omega L_g (i_{od} + ji_{oq}) = -\omega L_g i_{oq} + j\omega L_g i_{od} \tag{9}$$

$$\begin{cases} V_{dLg} = -\omega L_g \cdot i_{oq} \\ V_{qLg} = \omega L_g \cdot i_{od} \end{cases} \tag{10}$$

From (10), the voltage drop in the d-axis is affected by the current in the q-axis, while the voltage drop in the q-axis is affected by the current in the d-axis. Likewise, the proposed virtual inductance in the d-q frame is shown as follows:

$$\begin{cases} \omega = \omega^* - mP - m_d \dfrac{dP}{dt} \\ v_{dref} = V_{ref} - nQ - n_d \dfrac{dQ}{dt} - (-X_v \dfrac{\omega_c}{s+\omega_c} i_{oq}) \\ v_{qref} = 0 - X_v \dfrac{\omega_c}{s+\omega_c} i_{od} \end{cases} \tag{11}$$

where X_v is the virtual impedance. Compared with the virtual inductance [6]-[8], [10]-[12], the proposed virtual inductance is more robust due to the elimination of differential computations. Since the virtual inductance is much larger than the actual line impedance, the line resistance can be negligible. The coupling between the active and reactive power is reduced. With the power sharing control based on (11), a good transient response and accurate load current sharing can be achieved. The proposed control strategy is applicable for inverter units with mismatched transmission line impedances.

B. Voltage and Current Control Loop

The control strategy for the output voltage and current control in Fig. 3 is detailed in Fig.5. As can be seen, v_d and v_q are the output voltages of the d-axis and the q-axis while i_d and i_q are the filtered inductor currents of the d-axis and the q-axis, respectively. $G_c(s)$ is the output voltage regulator while $G_i(s)$ is

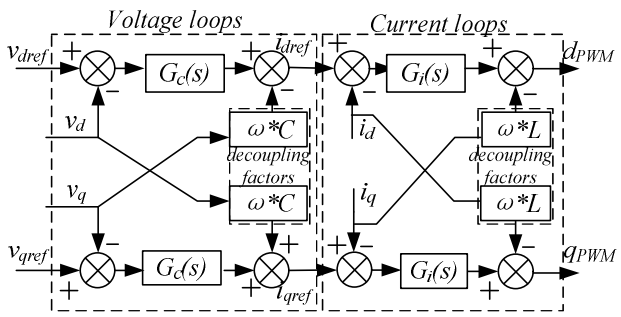

Fig. 5. Control strategy of the inverter under d-q frame.

the current regulator. L is the filter inductance and C is the filter capacitance. The outputs of the voltage loops work as current loop references. The phase angular used for the *d-q* transformation is derived by the integration of the angular frequency ω.

The outer voltage controller and the inner current controller are both implemented by *PI*. The outer controller is used to achieve voltage tracking. The inner current controller $G_i(s)$ should be designed with a high bandwidth to damp the resonance and improve the dynamic response.

IV. Modeling and Stability Analysis

Many models have been established for DG systems [8], [10], [13]. However, the line impedance is viewed as either fully inductive or fully resistive. A mathematical model is given in this paper for the viewing of general transmission line impedance. As shown in Fig.2, the output voltage of the inverter $\vec{E}$ in series with the line impedance $\vec{Z}$ connects to the common AC bus $\vec{V}$. In this figure, $\vec{E}$ is defined as $e_d + j \cdot e_q$. A small signal analysis is made to investigate the stability of the system. It should be noted that the analysis is made assuming that ϕ is very small. If the common AC bus $\vec{V}$ is a stiff AC source, the output current $i_{od}+j \cdot i_{oq}$ is obtained as follows:

$$\begin{aligned} i_{od} + j \cdot i_{oq} = \frac{\vec{E} - \vec{V}}{\vec{Z}} = \frac{1}{Z}[(e_d - V)\cos\theta + e_q \sin\theta] \\ - j \cdot \frac{1}{Z}[(e_d - V)\sin\theta - e_q \cos\theta] \end{aligned} \tag{12}$$

By linearizing (12), the small signal dynamic of i_{od} and i_{oq} are written by:

$$\begin{cases} \Delta i_{od} = \dfrac{1}{Z}(\Delta e_d \cdot \cos\theta + \Delta e_q \cdot \sin\theta) \\ \Delta i_{oq} = -\dfrac{1}{Z}(\Delta e_d \cdot \sin\theta - \Delta e_q \cdot \cos\theta) \end{cases} \tag{13}$$

Since:

$$p + j \cdot q = V \cdot (i_{od} + j \cdot i_{oq})^* = V \cdot i_{od} - j \cdot V \cdot i_{oq} \tag{14}$$

Linearizing (14) gives:

$$\begin{cases} \Delta p = V \cdot \Delta i_{od} = \dfrac{1}{Z}(V \cdot \Delta e_d \cdot \cos\theta + V \cdot \Delta e_q \cdot \sin\theta) \\ \Delta q = -V \cdot \Delta i_{oq} = \dfrac{1}{Z}(V \cdot \Delta e_d \cdot \sin\theta - V \cdot \Delta e_q \cdot \cos\theta) \end{cases} \tag{15}$$

Supposing that the output voltage achieves zero error tracking, thus $e_d=v_{dref}$ and $e_q=v_{qref}$. By linearizing (11), the dynamic of the proposed control strategy can be written as:

$$\begin{cases} \Delta\omega = -m \cdot \dfrac{\omega_c}{s+\omega_c}\Delta p - s \cdot m_d \dfrac{\omega_c}{s+\omega_c}\Delta p \\ \Delta e_d = -n \cdot \dfrac{\omega_c}{s+\omega_c}\Delta q - s \cdot n_d \cdot \dfrac{\omega_c}{s+\omega_c}\Delta q + X_v \dfrac{\omega_c}{s+\omega_c}\Delta i_{oq} \\ \Delta e_q = -X_v \dfrac{\omega_c}{s+\omega_c}\Delta i_{od} \end{cases} \tag{16}$$

Since $\Delta\omega = s\Delta\phi$, substituting (15) into (16) yields:

$$\begin{cases} \ddot{\Delta\phi} + \omega_c \cdot \dot{\Delta\phi} = -m \cdot \omega_c \cdot \Delta p - m_d \cdot \omega_c \cdot \dot{\Delta p} \\ \dot{\Delta e_d} + \omega_c \cdot \Delta e_d = -n \cdot \omega_c \cdot \Delta q - n_d \cdot \omega_c \cdot \dot{\Delta q} + X_v \cdot \omega_c \cdot \Delta i_{oq} \\ \dot{\Delta e_q} + \omega_c \cdot \Delta e_q = -X_v \cdot \omega_c \cdot \Delta i_{od} \end{cases} \tag{17}$$

where $\dot{}$ represents the first-order derivative and $\ddot{}$ is the second-order derivative. In addition:

$$\phi = \arctan(e_q / e_d) \tag{18}$$

Linearizing ϕ yields:

$$\Delta\phi = -e_q \Delta e_d / (e_d^2 + e_q^2) + e_d \Delta e_q / (e_d^2 + e_q^2) \tag{19}$$

Rearranging (17) leads to:

$$\Delta e_q = \frac{e_d^2 + e_q^2}{e_d} \cdot \Delta\phi + \frac{e_q}{e_d} \cdot \Delta e_d \tag{20}$$

Based on (13), (15), (17) and (20), the state space equation for the system is written as:

$$\begin{bmatrix} \dot{\Delta\phi} \\ \ddot{\Delta\phi} \\ \dot{\Delta e_d} \end{bmatrix} = \begin{bmatrix} 0 & 1 & 0 \\ f & -\omega_c & e \\ d & 0 & c \end{bmatrix} \begin{bmatrix} \Delta\phi \\ \dot{\Delta\phi} \\ \Delta e_d \end{bmatrix} \tag{21}$$

The related coefficients are expressed as follows:

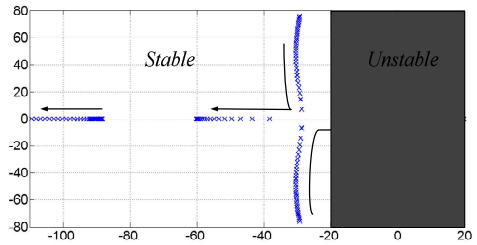

Fig. 6. Root locus of the system with various X_v.

TABLE I
SIMULATION PARAMETERS

V	380V
e_d+j·e_q	370+j30V
ω_c	60 rad/s
Z	0.54 Ω
m	68.2°
n	1×10^{-3}
m_d	1×10^{-2}
n_d	1×10^{-5}
$G_i(s)$	1×10^{-4}
$G_c(s)$	13+100/s
	0.1+50/s

$$
\begin{cases}
a = -\dfrac{X_v\omega_c\cos\theta}{Z} + (-\omega_c - \dfrac{X_v\omega_c\sin\theta}{Z})\dfrac{e_q}{e_d} \\
b = (-\omega_c - \dfrac{X_v\omega_c\sin\theta}{Z})\dfrac{e_d^{\,2}+e_q^{\,2}}{e_d} \\
c = \dfrac{Z}{Z+n_d\omega_c V\sin\theta}(-\omega_c - \dfrac{n\omega_c V\sin\theta}{Z} + \dfrac{n\omega_c V\cos\theta}{Z}\cdot\dfrac{e_q}{e_d} \\
\quad - \dfrac{X_v\omega_c\sin\theta}{Z} + \dfrac{X_v\omega_c\cos\theta}{Z}\cdot\dfrac{e_q}{e_d} + \dfrac{n_d\omega_c V\cos\theta}{Z}\cdot a) \\
d = \dfrac{Z}{Z+n_d\omega_c V\sin\theta}[\dfrac{n\omega_c V\cos\theta}{Z}(\dfrac{e_d^{\,2}+e_q^{\,2}}{e_d}) \\
\quad + \dfrac{n_d\omega_c V\cos\theta}{Z}\cdot b + \dfrac{X_v\omega_c\cos\theta}{Z}(\dfrac{e_d^{\,2}+e_q^{\,2}}{e_d})] \\
e = -\dfrac{m\omega_c V\cos\theta}{Z} - \dfrac{m\omega_c V\sin\theta}{Z}\cdot\dfrac{e_q}{e_d} - \dfrac{m_d\omega_c V\cos\theta}{Z}\cdot c \\
\quad - \dfrac{m_d\omega_c V\sin\theta}{Z}\cdot a \\
f = -\dfrac{m\omega_c V\sin\theta}{Z}\cdot(\dfrac{e_d^{\,2}+e_q^{\,2}}{e_d}) - \dfrac{m_d\omega_c V\cos\theta}{Z}\cdot d \\
\quad - \dfrac{m_d\omega_c V\sin\theta}{Z}\cdot b
\end{cases}
\tag{22}
$$

Equ. (21) represents the state space equation of the system as $\dot{X} = AX$. The droop control can be designed according to the desired voltage quality. The parameter design for the droop control is given in [3], [10], and [13]. This paper focuses on the virtual inductance design. To analyze the stability of the system, the characteristic equation $|sI - A| = 0$ shows the system root location. The root locus with X_v increasing is shown in Fig.6. Considering the power level of the system and the distortion of the output voltage, the droop coefficients are designed properly and the other parameters are shown in Table I. With X_v increasing, the complex-conjugate dominant eigenvalues move towards the real axis, which increases the damping factor. The overshoot during the dynamic response is mitigated. By further increasing X_v, the complex-conjugate dominant eigenvalues intersect at the real axis, causing the system over damped. If the value of X_v is too large, the dominant eigenvalue moves from the left side of the plane to the right side, which results in instability. In order to ensure the stability and to share the load current among the inverter units, the virtual inductance should be designed to satisfy the desired damping performance. Fig. 7 shows the simulation results with different values of X_v. In order to verify the effectiveness, the transmission line impedances of the two units are chosen with a 30% mismatch. From Fig. 7 (a) and (b), it can be seen that the load current sharing accuracy can be enhanced and the dynamic performance of the system can be effectively improved with the virtual inductor X_v increasing. However, as can be seen in Fig. 7 (c), the system is unstable when a value of X_v is chosen that is beyond the stability range.

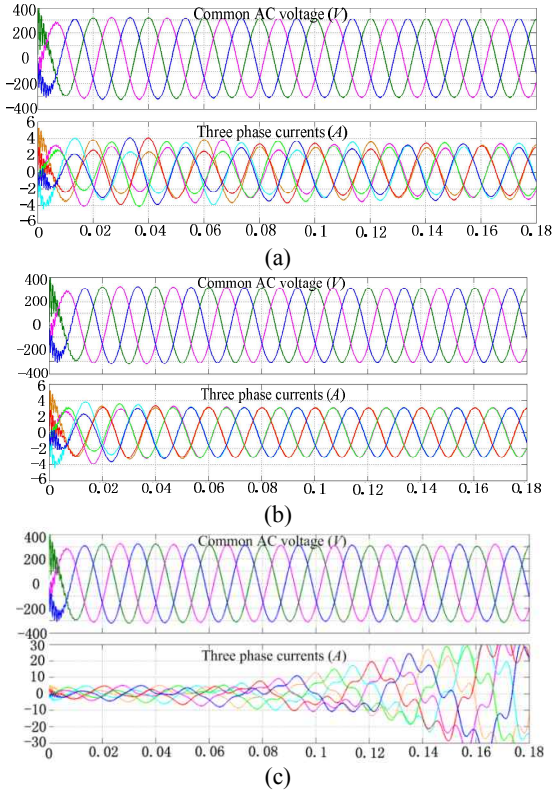

Fig. 7. Simulation results of the system with different value of X_v (a) X_v=0 (b) X_v=1 (c) X_v=2.

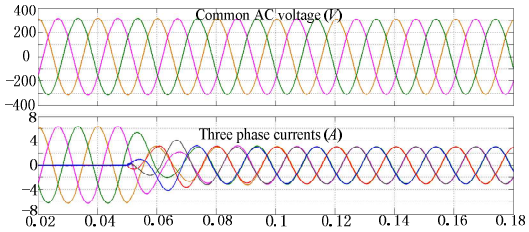

Fig. 8. Simulation result when inverter #2 is inserted.

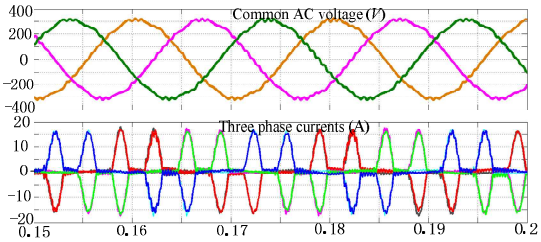

Fig. 9. Simulation result under a nonlinear load.

V. Simulation and Experimental Results

The simulation results of two paralleled inverters are shown in Fig. 8 and Fig. 9. Fig. 8 shows the dynamic response when another inverter is inserted. Before inverter #2 is added, the PLL is implemented by inverter #2. With the proposed control strategy, the system operates smoothly and the circulating current is effectively eliminated.

Fig. 9 shows the simulation result under a nonlinear rectifying load. As can be seen, the load current is shared almost equally between the two units.

A microgrid system composed of two 1.5-kVA three-phase inverters is built to verify the effectiveness of the proposed control strategy. The experimental results are shown in Fig.10 to Fig. 14. The switching frequency is 5 kHz, the input dc voltage of the inverter is 600V and the output line-to-line voltage is 380V. In the experiments, the parameters of the LC filter are: L=2 mH, C=30 μF. A TMS320F2812 digital controller is used to implement the control strategy. The parameters of the current loop controller and the voltage loop controller are the same as the parameters shown in the simulation. The droop coefficients are: m=1×10^{-3}, n=1×10^{-2}, m_d=2×10^{-5}, n_d=1×10^{-4}, and X_v=0.5.

Fig. 10 shows the currents of the individual inverters when inverter #2 is inserted. As inverter #2 is connected to the system, the currents of inverter #1 decrease gradually and the currents of inverter #2 increase at the same time. As can be seen from the waveform, with the proposed control strategy there is no overshoot when inverter #2 is added. After several fundamental periods, the system operates in the steady state and the two inverter units share the load current.

Fig. 11 shows the common voltage source v_{ab} and the individual currents of phase a, when inverter #2 is added. As can be seen, the dynamic response is excellent. The common voltage source v_{ab} is almost unaffected while inserting inverter #2. Fig. 12 shows the common voltage v_{ab} and the individual load currents of phase a under linear loads, which shows good current sharing under the steady state.

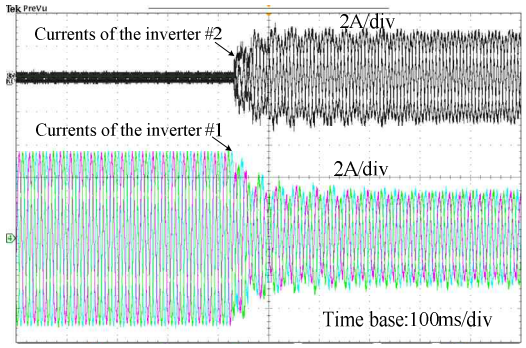

Fig. 10. Dynamic response of the individual three-phase currents when the inverter #2 is inserted.

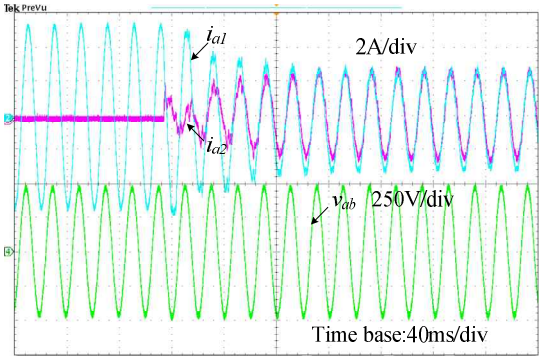

Fig. 11. Dynamic response of $\boldsymbol{v_{ab}}$ and the individual currents of phase $\boldsymbol{a}$ when the inverter #2 is inserted under linear loads.

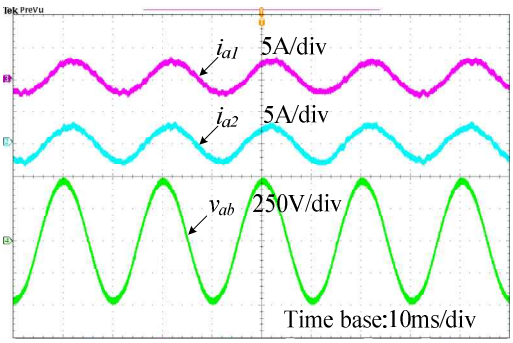

Fig. 12. Steady state waveforms under a linear load.

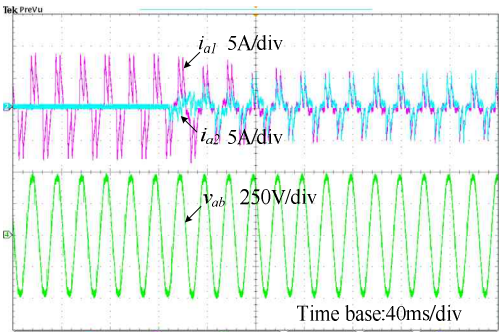

Fig. 13. Dynamic response under a rectifier load.

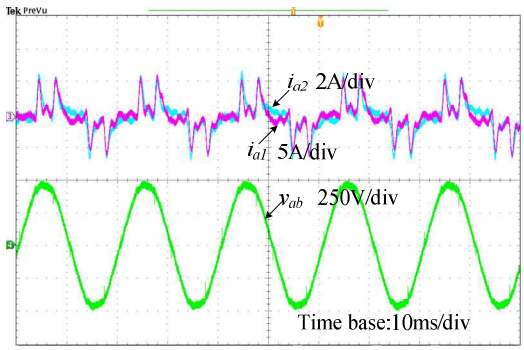

Fig. 14. Steady state waveform under a rectifier load.

Fig. 13 shows the common voltage source v_{ab} and the individual currents of phase *a* under a nonlinear rectifier load with a 1000 μF capacitor paralleled with a 100 Ω resistor when inverter #2 is connected to the system. As can be seen, a good dynamic response can be achieved under a rectifier load. Fig. 14 shows the common voltage source v_{ab} and the individual currents of phase *a* under the steady state. Good current sharing can be obtained under a rectifier load. Therefore, the proposed control strategy is perfectly suitable for linear and nonlinear loads.

.

VI. CONCLUSIONS

This paper presents a method of sharing the output current among paralleled inverters suitable for DG systems. A virtual inductor implementation in the synchronous *d-q* frame is proposed. With this scheme, the output current is perfectly shared among the inverters for both linear and nonlinear loads. By avoiding the use of differential calculations, the control strategy is much more robust. The method of the virtual reactance design is given in view of its stability, damping and dynamic performance. A model is proposed for the design of the control system and simulations of the two inverter units are made. Experimental results on a distributed generation system composed of two 1.5-kVA inverter units validate the effectiveness of the control strategy.

ACKNOWLEDGEMENT

This work was supported by National Nature Science Foundation of China under Grant 50807005, by Beijing Natural Science Foundation under Grant 3132032, by the Excellent Young Scholars Research Fund of Beijing Institute of Technology under Grant 2010YC0604 and by the Fundamental Research Fund of Beijing Institute of Technology under Grant 20120642009.

REFERENCES

[1] Y. Mohamed and E. El-Saadany, "Adaptive decentralized droop controller to preserve power sharing stability of paralleled inverters in distributed generation microgrids," *IEEE Trans. Ind. Electron.*, Vol. 23, No. 6, pp. 2806-2816, Nov. 2008.

[2] Y. Li, D. M. Vilathgamuwa, and P. Loh, "Design, analysis, and real-time testing of a controller for multibus microgrid system," *IEEE Trans. Power Electron.*, Vol. 19, No. 5, pp. 1195- 1204, Sep. 2004.

[3] M. Marwali, J. Jung, and A. Keyhani, "Control of distributed generation systems—part II: load sharing control," *IEEE Trans. Power Electron.*, Vol. 19, No. 6, pp. 1551-1561, Nov. 2004.

[4] C. Chen, Y. Wang, J. Lai, Y. Lee, and D. Martin, "Design of parallel inverters for smooth mode transfer microgrid applications," *IEEE Trans. Power Electron.*, Vol. 25, No. 1, pp 6-15, Jan. 2010.

[5] H. Cai, R. X. Zhao, and H. Yang, "Study on ideal operation status of parallel inverters," *IEEE Trans. Power. Electron.*, Vol. 23, No. 6, pp. 2964 -2969, Nov.2008.

[6] J. Guerrero, L. Vicuña, J. Matas, M. Castilla, and J. Miret, "A wireless controller to enhance dynamic performance of parallel inverters in distributed generation systems," *IEEE Trans. Power Electron.*, Vol. 19, No. 5, pp. 1205-1213, Sep. 2004.

[7] J. Guerrero, J. Vasquez, J. Matas, L. Vicuna, and M. Castilla, "Hierarchical control of droop-controlled AC and DC microgrids – A general approach toward standardization," *IEEE Trans. Ind. Electron.*, Vol. 58, No. 1, pp. 158-172, Jan. 2011.

[8] J. Guerrero, J. Matas, L. Vicuña, M. Castilla, and J. Matas, "Decentralized control for parallel operation of distributed generation inverters using resistive output impedance," *IEEE Trans. Ind. Electron.*, Vol. 54, No. 2, pp. 994-1004, Apr. 2007.

[9] U. Borup, F. Blaabjerg, and P. Enjeti, "Sharing of nonlinear load in parallel-connected three-phase converters," *IEEE Trans. Ind. Applicat.*, Vol. 37, No. 6 pp. 1817-1823, Nov. 2001.

[10] J. Guerrero, J. Matas, L. Vicuna, M. Castilla, J. Miret, "Wireless-control strategy for parallel operation of distributed-generation inverters," *IEEE Trans. Ind. Electron.*, Vol. 53, No. 5, pp. 1461-1470, Oct. 2006.

[11] J. Guerrero, J. Vásquez, J. Matas, M. Castilla, and L. Vicuna, "Control strategy for flexible microgrid based on parallel line-interactive ups systems," *IEEE Trans. Ind. Electron.*, Vol. 56, No. 3, pp. 1461-1470, Mar. 2009.

[12] J. Guerrero, L. Vicuña, J. Matas, M. Castilla, and J. Miret, "Output impedance design of parallel-connected UPS inverters with wireless load-sharing control," *IEEE Trans. Ind. Electron.*, Vol. 52, No. 4, pp. 1126-1135, Aug. 2005.

[13] D. De, and V. Ramanarayanan, "Decentralized parallel operation of inverters sharing unbalanced and nonlinear loads," *IEEE Trans. Power Electron.*, Vol. 25, No. 12, pp. 3015-3025, Dec. 2010.

[14] X. Yu, Ashwin M. Khambadkone, H. Wang, and S. T. S. Terence, "Control of parallel-connected power converters for low-voltage microgrid – Part I: a hybrid control architecture," *IEEE Trans. Power Electron.*, Vol.25, No.12, pp.2962-2970, Dec. 2010.

[15] Charles K. Sao, and Peter W. Lehn, "Autonomous load sharing of voltage source converters," *IEEE Trans. Power Del.*, Vol. 20, No. 2, pp. 1009-1016, Apr. 2005.

[16] J. Guerrero, L. Hang, and J. Uceda, "Control of distributed uninterruptible power supply systems," *IEEE Trans. Ind. Electron.*, Vol. 55, No. 8, pp. 2845-2859, Aug. 2008.
[17] A. Tuladhar, Hua Jin, T. Unger, and K. Mauch, "Control of parallel inverters in distributed AC power systems with consideration of line impedance effect," *IEEE Trans. Ind. Applicat.*,Vol. 36, No.1, Jan./Feb. 2000.

Zhiqiang Guo was born in 1985. He received his B.S. in Automation from the Hebei University of Technology, Tianjin, China, in 2008, and his M.S. in Automatic Control from the Beijing Institute of Technology (BIT), Beijing, China, in 2010. He is currently pursing his Ph.D. in Electrical Automation at the Beijing Institute of Technology. His current research interests include power electronics converters and microgrid applications.

Deshang Sha was born in 1977. He received his B.S. from the Luoyang Institute of Technology, Luoyang, China, in 1998, his M.S. from the Nanjing University of Aeronautics and Astronautics, Nanjing, China in 2001, and his Ph.D. from the Institute of Electrical Engineering, Chinese Academy of Sciences, Beijing, China, in 2005, all in Electrical Engineering. From 2005 to 2007, he worked as the Head and Chief Engineer of the full-digitalized welding machine research department of Time Group Inc., Beijing, China. Since 2008, he has been with the School of Automation, Beijing Institute of Technology (BIT), Beijing, China, where he is currently an Associate Professor. From 2012 to 2013, he was a Visiting Scholar with the Future Energy Electronics Center (FEEC), Virginia Polytechnic Institute and State University, Blacksburg, Virginia. His current research interests include the modeling and control of power converters, high-efficiency power conversion, power electronics applications in renewable energy power generation systems and microgrid systems. Dr. Sha received an Excellent Yong Scholar Award of BIT in 2010.

Xiaozhong Liao was born in China, in 1962. She received her B.S. and M.S. in Electrical Engineering from Tianjin University, Tianjin, China, in 1982 and 1984, respectively, and her Ph.D. in Control Sciences and Engineering from the Beijing Institute of Technology (BIT), Beijing China, in 2004. She was a Visitor Researcher in the Department of Electrical and Electronic Engineering, University of Central Lancashire, Preston, U.K., form 1995 to 1996. She is currently an Associate Dean and Full Professor in the School of Automation, Beijing Institute of Technology. Her current research interests include power electronics, motor drives and renewable energy power conversion.